2023 IMEKO TC-4 International Conference on
Metrology for Archaeology and Cultural Heritage
Rome, Italy, October 19-21, 2023

Inorganic, organic and biochemical characterization of wall paintings from a Roman *domus*

Leila Birolo[1,2], Manuela Rossi[3], Miriam Alberico [1,4], Nunzia De Riso[1], Georgia Ntasi [1], Antonella Tomeo [5], Alessandro Vergara [1,2]

[1] *Dept. Chemical Sciences, University of Napoli Federico II, Via Cintia, Napoli*
[2] *Task Force "Metodologie Analitiche per la Salvaguardia dei Beni Culturali", University of Napoli Federico II, Via Cintia, Napoli*
[3] *Dept. Earth Sciences, Environment and Resources, University of Napoli Federico II, Via Cintia, Napoli*
[4] *Dip. Scienze dell'Antichità, Università la Sapienza, P.le Aldo Moro, Roma*
[5] *Soprintendenza Archeologia Belle Arti e Paesaggio per le Province di Caserta e Benevento, Reggia di Caserta, Caserta*

***Abstract* – Pigments, ligands, and mortars of wall paintings from a Roman *domus* in Santa Maria Capua Vetere were studied with a multi-methodological approach. Optical and Scanning Electron microscopy, Raman micro-spectroscopy were combined with GC-MS and LC-MS/MS analyses in order to achieve a comprehensive picture of the chemical components of some fine wall paintings recently excavated in Santa Maria Capua Vetere. The four-layers preparation, the rich pigments palette (both natural and synthetic ones) and the variety of the organic ligands used support the hypothesis of a very wealthy owner. The archaeological indication suggest that he might be related to the Emperor Augustus.**

KEYWORDS: wall paintings, pigments, ligands, proteomics

I. INTRODUCTION

The city of Santa Maria Capua Vetere is located in the ruins of ancient Capua, a city of Roman origin in southern Italy [1]. During Roman times the city lived a very prosperous era, rich enough to be called Campania felix. After the domination of the Osci and Etruscans, in 841 the city was almost destroyed by the incursions of the Saracens. Due to its history, the city can count on different archeological monuments such as: the Campano amphitheater, the arch of Hadrian, the *domus* (in Via degli Orti); although, many archaeological artifacts are still buried. In 2018 some excavations have unearthed a multi-level site consisting of a hypogeum and a Roman villa. In this work, several areas of the Roman villa have been investigated, the sampling includes wall paintings and mortars. The molecular characterization of the murals in terms of colors and/or organic binders can reveal important aspects about its conservation state [2-6]. Vibrational spectroscopies, optical and electronic microscopies and chromatographic techniques were used to identify the layers composing the wall painting, and a large variety of pigments and binders. The data obtained can give information on diagnostic of the components of the samples analyzed and their conservation state. Four fragments of wall paintings selected on site were analyzed (187, 151A, 151B, 151C) with special attention to pigments, binders and mortars.

II. RESULTS AND DISCUSSIONS

In 2018, a house dating back to the Roman era was excavated. Two fragments of the wall paintings 151 and 187 were selected on the site and analyzed with special attention to pigments, binders, and mortars. Due to its color complexity, the sample 151 was divided in three sections (151 A, 151 B, 151 C). All the samples were analyzed using a multi-methodological approach, which include optical and electronic microscopies, Raman micro-spectroscopy, GC-MS, and LC-MS/MS techniques.

A. Optical, electron microscopy and quantitative chemical analysis

The samples were analyzed in two different perspectives, the first is a macroscopic observation on 3D materials with a stereomicroscope, the second is a petrographic observation on thin section with the petrographic microscope. Moreover, the elemental analysis of the samples analyzed was performed with SEM-EDS. The

samples are wall fragments generally composed of three layers, that have different thickness, textures, and mineralogical compositions.

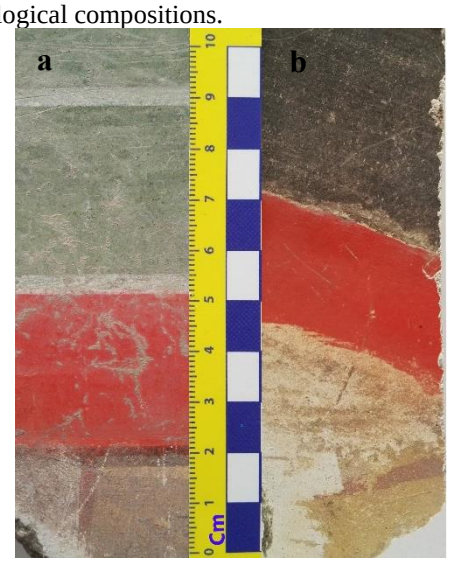

Fig. 1. The different colors that compose the first level of the samples 151(a) and 151C(b).

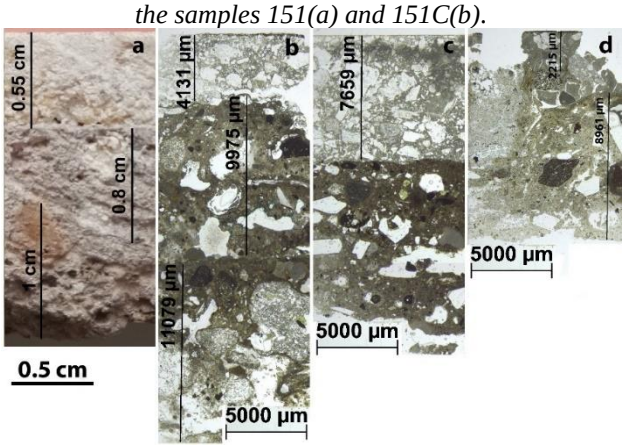

Fig. 2. The different layers, including the pictorial level and the mortars of samples: 151C sample (a); thin section in SM of 151C sample (b), 151 sample (c) and 187 sample (d).

Based on SM and PM observations, the fragments are generally composed of three layers. The first layer consists in a pictorial level with variable colors (level 1; figure 1), the second layer has a very light color and shows binder mixed to crystals fragments at first sight (level 2; figure 2a, b, c and d), the third layer is characterized by a brownish binder mixed to volcanic fragments (scoriae, pumices and crystals) with different dimensions (level 3; figure 2c), probably pozzolanic mortar.

Generally, the level 1 has a variable thickness between 200 µm and 11 µm with different, sometimes overlapping, colors. The most common color is red, in various shades, but there are also green, in various shades, yellow, black, and a very light pink as well as white slightly yellowed. Often the same sample has different colors simultaneously (Figure 1).

The portions of the frescoed walls analyzed present locally incrustations of different materials (patinas alteration of pictorial levels, soil, etc; figure 1) and/or profound incisions sometimes parallel to each other, in other cases there are holes of different depths and extensions (Figure 1), in which the layer of paint has been completely removed.

After a careful analysis with petrographic microscope and EDS analyses, the pictorial layers are characterized by the presences of cryptocrystalline and microcrystalline minerals associated to minor amount of cryptocrystalline lime binder. The pictorial layers characterized by a reddish color, often tending to reddish/brown or yellow, appear respectively composed of cryptocrystalline goethite (α-$Fe^{3+}O(OH)$) associated to microcrystals of hematite (Fe_2O_3) and of cryptocrystalline Fe and Pb oxides and hydroxides, while the layers of bright red color are mainly made up of cryptocrystalline and microcrystalline cinnabar (HgS) and hematite In particular, the reddish/brown pictorial levels appear composed by 80-90% of goethite and 20-10% of hematite; the bright red levels are composed by 90% cinnabar and 10% of hematite and the yellow pictorial layer is composed by Fe and Pb hydroxides with variable amount of PbO between 33,6wt% and 1,19wt%.

The green pigments are mainly made up of a strongly pleochroic mineral, with colors varying from light and darker green to turquoise. The green color is typical of glauconite $(K,Na)(Mg,Fe^{2+},Fe^{3+})(Fe^{3+},Al)(Si,Al)_4O_{10}(OH)_2$) and/or chlorite (clinochlore ($Mg_5Al(AlSi_3O_{10})(OH)_8$) [7, 8]. The blue fragments, on the other hand, are weakly pleochroic with turquoise colors of variable intensity. These turquoise crystals also have strong birefringence and high interference colors, all typical characteristics of copper-rich silicate minerals. Quantitative chemical analyses confirmed the presence of glauconite while for turquoise crystals they showed the presence of cuprorivaite ($CaCuSi_4O_{10}$); the glauconite crystals are most abundant. The white sample mainly consist of micro crystals of calcium carbonate.

The second layer (level 2), most likely the preparation layer, is white-grey colored, and its thickness varies from 4 to 8 mm. In a thin section it appears to be composed of a fine matrix in which are immersed calcite ($CaCO_3$) crystals of highly variable dimensions. Only in the sample 187 the crystals appear to consist also of dolomite ($CaMg(CO_3)_2$).

Level 3 seems to be composed of a pyroclastic rock fragment in a lime binder, a composition similar to s*cratch coat layers of plasters* [9]. The microscopic observation shows the presence of fragments of altered pumice, minerals of feldspar group, plagioclase, clinopyroxene, mica, strongly altered leucite, apatite minerals group and oxides in smaller quantities. Elemental analyses have been of fundamental importance to confirm the hypothesis of the presence of *scratch coat layers*, in fact they have highlighted the presence of calcium carbonate in the

binder, even if it had variable silicon contents up to 8%. Level 4 was only detected in one sample. It appears to be constituted by pumice and glass immersed in a darker matrix. Chemical analyses have shown that the matrix has a silicate component of up to 18%, while the rest of the matrix continues to be made up of calcium carbonate, it could be bedding mortars [10].

B. Raman micro-spectroscopy

Only the pictorial layers (first level) of the samples were investigated by Raman spectroscopy for pigment analysis (samples 187, 151A, 151B, 151C, Figure 3). The samples consist of well-preserved colored fragments of red, yellow, blue, green, and white. The Raman spectra demonstrated blue color of the sample 151A exhibit Raman peaks at 1089 cm^{-1} and 430, 467, 572, 757, 989, 1015, 1087 cm^{-1}, respectively assigned to *Carbonate* (Figure 3, trace 7) [11, 12] and *Cuprorivaite* ($CuSi_4O_{10}$) famous as Egyptian blue (Figure 3, trace 1) [13, 14]. Green color of the sample 151A shows signals belonging to the "Green earths" attributable to Glauconite (Figure 3, trace 3). The samples 151A, 151B and 151C show different shades of red. The red spot belonging to 151A shows very strong signals at 254, 287 and 344 cm^{-1}, easily assigned to HgS (Figure 3, trace 2) [15, 16], while both the red spot of 151B and 151C show a tonality resulted from several components. Both of them show signals attributable to both Hematite and Goethite (Figure 3, trace 8) [17, 18], the main difference is in the presence of a third component in the sample 151 B diagnosed by a signal at 1296 cm^{-1} a signal at 1611 cm^{-1} of lower intensity that can be assigned to amorphous carbon (Figure 3, trace 6) [17, 18]. Here, the inversion of intensity between the D and G bands of coal is due to the overlap of the latter with Hematite. It must be pointed out that the Goethite was not detected by SEM analysis. In fact, it is difficult to distinguish between the two iron compounds using this kind of analysis except than for pure phases of the minerals.

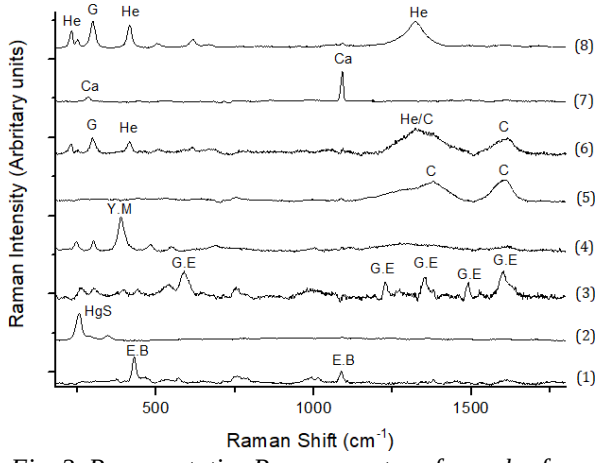

Fig. 3. Representative Raman spectra of samples from S.M. Capua Vetere. He (hematite); C (carbon); Ca (carbonate); E.B (Egyptian blue); G.E (Green earths); HgS (Cinnabar); G (Goethite).

This might be probably caused by a partial "Goethite-Hematite" conversion, possibly due to the laser exposure [17, 20, 21]. It is worth noting that most likely goethite itself is a product of oxidation of an initial hematite, so accidentally the laser-induced Raman assignment can correspond to the actual starting pigment.

The white spot of the 151 C sample can be easily assigned as carbonate (Figure 3, trace 7) because of the peaks at 285 and 1091 cm^{-1}, however the latter could also be a component of the second layer and not of the first one. The yellow spot of the sample 151 B exhibits Raman bands typical of $Fe(OH)_3$ (Figure 3, trace 4) [22]. In this case, Raman analysis only reveals one minor component of the pigment, in fact the elemental analysis of the yellow pigments is highly heterogeneous most likely corresponding to the limonite (mixture of hydroxide/oxides of iron, zinc and titan). Although the spectra of samples 187 do not show Raman bands of any pigments, they are characterized by trace of β-carotene, indicating a poor biodeterioration of the pictorial layer [23].

C. GC-MS: analysis of organic binders

A multistep protocol was applied to all samples of wall paintings to separate the polar fractions, that include sugars and compounds of medium polarity, from the unpolar fraction composed mainly of lipids. The polar fraction was subjected to sugar analysis and chemical derivatization with TMS, whereas the unpolar fraction was subjected to transesterification and GC-MS analysis. No sugars were detected in any sample but instead, flavonoids, steroids, compounds with abietanic skeleton were identified. In all samples, diglycidyl bisphenol A that is a characteristic organic compound of epoxy resins [24] and 10,18-bisnorabieta-8,11,13-triene that is a degradation product of abietic acid [25, 26], were detected. The co-presence of these compounds illustrates the use of epoxy resins as organic binder. More specifically, the samples 151 A and 151 B show a similar chemical profile, with the presence of steroid compounds (Cholest-5-en-19-al,3ß-hydroxy-,cyclic ethylene mercaptal, acetate and hexastrol) that are mostly detected in species of animal origin [27], thus suggesting the presence of an organic binder. On the other hand, stephaboline in the sample 151 C and the semi-long fatty acids that were detected in sample 187 are chemical compounds that are found in plants [28, 29]. Moreover, several fatty acids were detected as methyl ester derivatives (FAMEs) in the unpolar fractions. In particular, palmitic and stearic acid, two of the most common molecules that can be found in many matrices both of animal and vegetable origin, were detected in all samples. The relative ratio is affected by aging. Based on the literature data [30], the ratio C16:0/C18 in the samples 151 A and 151 B is compatible with the presence of animal fat, although in the samples 151 C and 187 is not clearly ascribable to animal or vegetable fat.

D. LC-MS/MS: analysis of proteinaceous binders

A classical proteomic approach in heterogeneous phase was performed to investigate the presence of proteinaceaous binders. Initially, proteins were identified searching SwissProt database, with all entries as taxonomy restriction, with MS/MS Ion search Mascot software (Matrix Science). When collagen was detected, the sample was reanalyzed against a homemade collagenous database, "COLLE" (60 sequences; 88859 residues). Deamidation of Gln and Asn, oxidation on Met, hydroxylation (K) and hydroxylation (P) were set as variable modifications. In the samples 151 A and 151 B collagen chains of type I of *Bos taurus* were detected, supporting the hypothesis of lipids from an animal origin. No significant proteins were detected in the samples 151C and 187.

Proteomic data were also used for a different type of study. According to the literature, there are some bacteria capable of producing pigment with different varieties of colors [31, 32]. For example, the bacteria *Flavobacterium sp* produces a yellow-creamy color although the *Chromobacterium violaceum* a red color. We thought that these bacteria could in case of a historical painting be produced using the sugars coming from the resins or the natural gums used for the color protection in the wall surface, thus providing another color source. Therefore, to further validate that the colors observed are not result of a bacteria production, the proteomic data were analyzed against a protein database containing the protein sequences of bacteria, capable to produce intense colors (18191sequences; 6393558 residues).

III. CONCLUSIONS

Raman and SEM spectroscopy analyses allowed to characterize the inorganic components of the different layers of the wall paintings of the Domus in S.M. Capua Vetere. The blue shade identified in the samples as "Egyptian *Blue*" [13, 14], is a concise pigment based on Cuprorivaite. The green color is Glauconite [7] known as "Green Earth". The elemental analysis of the yellow pigments indicates that they are highly heterogeneous, most likely corresponding to the mineral limonite (mixture of hydroxide/oxides of iron, zinc and titan), and Raman analysis revealed one minor component, assigned as $Fe(OH)_3$ [22]. The Raman results for the *red* shade confirms the presence of HgS in the "151 A" sample, while the "151 B" and the "151 C" shows the co-presence of Goethite and Haematite [15-18]. The complex mortars preparation (that goes from three to four layers) results of raw material blends, as shown from the optical microscopy and the abundance of binder suggests that the villa is an aristocratic one [1].

These observations were confirmed by the analysis of the organic component. In the preparation of the wall paintings, resins and animal glue have been extensively used, so they can be classified as fresco-secco paintings, where the color was applied directly on dry mortar [33]. In the Roman period this technique was less common in comparison to fresco where the painting preparation does not include the use of a proteinaceous binder but instead the use of emulsified beeswax. Interestingly, the observed colors are not related to degradation processes that involve bacteria, as confirmed by a screening of the proteomic data obtained against a database of bacteria that can produce colored pigments.

ACKNOWLEDGEMENTS

This work was financially supported by PNRR PE5 CHANGES (PE00000020).

REFERENCES

[1] M. Pagano, A. Tomeo, Capua la seconda Roma. Nuovi studi e ricerche, Belle Epoque Edizioni, **2021**. EAN 9788894302790.

[2] J. Cuní, P. Cuní, B. Eisen, R. Savizky, J. Bové, Characterization of the binding medium used in Roman encaustic paintings on wall and wood, Anal. Methods. 4 (2012) 659–669

[3] M. Gelzo, M. Grimaldi, A. Vergara, V. Severino, A. Chambery, A. Dello Russo, C. Piccioli, G. Corso, P. Arcari, Comparison of binder compositions in Pompeian wall painting styles from Insula Occidentalis, Coke Chem. 8 (2014) 65.

[4] G. Corso, M. Gelzo, A. Chambery, V. Severino, A. Di Maro, F.S. Lomoriello, O. D'Apolito, A. Dello Russo, P. Gargiulo, C. Piccioli, P. Arcari, Characterization of pigments and ligands in a wall painting fragment from Liternum archaeological park (Italy), J. Sep. Sci. 35 (2012) 2986–2993.

[5] A. Casoli, S. Santoro, Organic materials in the wall paintings in Pompei: A case study of Insula del Centenario, Chem. Cent. J. 6 (2012) 107.

[6] J. Cuní, What do we know of Roman wall painting technique? Potential confounding factors in ancient paint media analysis, Herit. Sci. 4 (2016) 44.

[7] Ugo Zezza, Petrografia microscopica , La Goliardica Pavese, 1976.

[8] A.P.D. Peccerillo, Introduzione alla petrografia ottica. , Morlacchi Editore, 2003.

[9] F. Izzo, A. Arizzi, P. Cappelletti, G. Cultrone, A. De Bonis, C. Germinario, S. F. Graziano, C. Grifa, V. Guarino, M. Mercurio, V. Morra, A. Langella (2016) The art of building in the Roman period (89 B.C. – 79 A.D.): Mortars, plasters and mosaic floors from ancient Stabiae (Naples, Italy). Construction and Building Materials 117 (2016) 129–143

[10] C. Rispoli, R. Esposito, L. Guerriero and P. Cappelletti Ancient Roman Mortars from Villa del Capo di Sorrento: A Multi-Analytical Approach to Define Microstructural and Compositional Features.

Minerals, (2021) 11, 469
[11] L. Birolo, A. Tomeo, M. Trifuoggi, F. Auriemma, L. Paduano, A. Amoresano, R. Vinciguerra, C. De Rosa, L. Ferrara, A. Giarra, A. Luchini, C. De Maio, G. Greco, A. Vergara, A hypothesis on different technological solutions for outdoor and indoor Roman wall paintings, Archaeol. Anthropol. Sci. 9 (2017) 591–602.
[12] S. Gunasekaran, G. Anbalagan, S. Pandi, Raman and infrared spectra of carbonates of calcite structure, J. Raman Spectrosc. 37 (2006) 892–899.
[13] H.M. Mahmoud, A multi-analytical approach for characterizing pigments from the tomb of djehutyemhab (TT194), elqurna necropolis, Upper Egypt, Archeometriai Muhely 9 (3) (2012) 205-214
[14] H.H. Marey Mahmoud, M. Mahmoud, H. H., A Preliminary Investigation Of Ancient Pigments From The Mortuary Temple Of Seti I, El-Qurna (Luxor, Egypt), MAA. 11 (2011) 99–106.
[15] R.J.H. Clark, P.J. Gibbs, K.R. Seddon, N.M. Brovenko, Y.A. Petrosyan, Non-destructive in situ identification of cinnabar on ancient Chinese manuscripts, J. Raman Spectrosc. 28 (1997) 91–94.
[16] P. Baraldi, C. Baraldi, R. Curina, L. Tassi, P. Zannini, A micro-Raman archaeometric approach to Roman wall paintings, Vib. Spectrosc. 43 (2007) 420–426.
[17] E.A. Lalla, G. Lopez-Reyes, A. Sansano, A. Sanz-Arranz, J. Martínez-Frías, J. Medina, F. Rull-Pérez, Raman-IR vibrational and XRD characterization of ancient and modern mineralogy from volcanic eruption in Tenerife Island: Implication for Mars, Geosci. Front. 7 (2016) 673–681.
[18] M. Alfè, V. Gargiulo, R. Di Capua, F. Chiarella, J.N. Rouzaud, A. Vergara, A. Ciajolo, Wet chemical method for making graphene-like films from carbon black, ACS Appl. Mater. Interfaces. 4 (2012) 4491–4498.
[19] D.C. Smith, M. Bouchard, M. Lorblanchet, An initial Raman microscopic investigation of prehistoric rock art in caves of the Quercy District, S. W. France, J. Raman Spectrosc. 30 (1999) 347–354.
[20] D.L.A. De Faria, S. Venâncio Silva, M.T. De Oliveira, Raman microspectroscopy of some iron oxides and oxyhydroxides, J. Raman Spectrosc. 28 (1997) 873–878.
[21] S. Das, M.J. Hendry, Application of Raman spectroscopy to identify iron minerals commonly found in mine wastes, Chem. Geol. 290 (2011) 101–108.
[22] I.M. Bell, R.J.H. Clark, P.J. Gibbs, Raman spectroscopic library of natural and synthetic pigments (pre- ≈ 1850 AD), Spectrochim. Acta Part A Mol. Biomol. Spectrosc. 53 (1997) 2159–2179.
[23] J. Jehlička, H.G.M. Edwards, K. Osterrothová, J. Novotná, L. Nedbalová, J. Kopecký, I. Němec, A. Oren, Potential and limits of Raman spectroscopy for carotenoid detection in microorganisms: Implications for astrobiology, Philos. Trans. R. Soc. A Math. Phys. Eng. Sci. 372 (2014).
[24] N. Szczepańska, P. Kubica, B. Kudłak, J. Namieśnik, A. Wasik, Stabilities of bisphenol A diglycidyl ether, bisphenol F diglycidyl ether, and their derivatives under controlled conditions analyzed using liquid chromatography coupled with tandem mass spectrometry, Anal. Bioanal. Chem. 411 (2019) 6387–6398.
[25] C. Azemard, M. Menager, C. Vieillescazes, Analysis of diterpenic compounds by GC-MS/MS: contribution to the identification of main conifer resins, Anal. Bioanal. Chem. 408 (2016) 6599–6612.
[26] V. Beltran, N. Salvadó, S. Butí, T. Pradell, Ageing of resin from Pinus species assessed by infrared spectroscopy, Anal. Bioanal. Chem. 408 (2016) 4073–4082.
[27] G. Kaklamanos, G. Theodoridis, T. Dabalis, Determination of anabolic steroids in bovine urine by liquid chromatography-tandem mass spectrometry, J. Chromatogr. B Anal. Technol. Biomed. Life Sci. 877 (2009) 2330–2336.
[28] H. Zhang, J.M. Yue, Hasubanan type alkaloids from Stephania longa, J. Nat. Prod. 68 (2005) 1201–1207.
[29] P. Ranchana, M. Ganga, M. Jawaharlal, M. Kannan, Investigation of Volatile Compounds from the Concrete of Jasminum auriculatum Flowers, Int.J.Curr.Microbiol.App.Sci. 6 (2017) 1525–1531.
[30] J. Blaško, R. Kubinec, B. Husová, P. Přikryl, V. Pacáková, K. Štulík, J. Hradilová, Gas chromatography/mass spectrometry of oils and oil binders in paintings, J. Sep. Sci. 31 (2008) 1067–1073.
[31] H.M. Usman, N. Abdulkadir, M. Gani, H.M. Maiturare, Bacterial pigments and its significance, (2017).
[32] P. Sabbagh, A. Ebrahimzadeh Namvar, The eminence status of bacterial pigments under different aspects, Microbiol. Medica. 32 (2017).
[33] M.A. Lozano-Grande, S. Gorinstein, E. Espitia-Rangel, G. Dávila-Ortiz, A.L. Martínez-Ayala, Plant Sources, Extraction Methods, and Uses of Squalene, Int. J. Agron. 2018 (2018).
[34] Koestler, R.J., Koestler, V.H., Elena Charola, A., Nieto-Fernandez, F.E., Art, Biology, and Conservation: Biodeterioration of Works of Art. The metropolitan museum of art, 2003.